

Surface Recombination Kinetics at the GaAs/Electrolyte Interface via Photoluminescence Efficiency Measurements

John F. Kauffman,* Chang Sheng Liu, and Maurice W. Karl

Department of Chemistry, University of Missouri, 123 Chemistry Building, Columbia, Missouri 65211

Received: January 7, 1998; In Final Form: May 11, 1998

Photoluminescence from GaAs/electrolyte junctions can provide detailed information concerning the kinetics of surface recombination. Here we present the results of a study of picosecond laser excited photoluminescence from the n-GaAs/Na₂S electrolyte junction. We have developed a model for the dependence of the photoluminescence efficiency (PLE) on the surface minority carrier trapping rate following photoexcitation with a short light pulse. The model indicates that the functional dependence of the PLE on the surface minority carrier trapping rate is identical to that under CW excitation. The PLE from the n-GaAs/Na₂S junction is shown to depend strongly on the excitation intensity, which we attribute to surface trap state filling. We have used our model to measure the surface minority trapping velocity as a function of excitation power at the flat band potential. From these measurements we conclude that the residence time of minority carriers within the trap states is on the order of microseconds, which is 3 orders of magnitude longer than the bulk minority carrier lifetime.

I. Introduction

Surface midgap states localized at the semiconductor/electrolyte interface can have a profound effect on the dynamics of photoexcited carriers.^{1–7} Minority carrier trapping is the primary mechanism by which dynamics are influenced. Surface minority carrier trapping with subsequent electron–hole recombination is often a dominant loss mechanism which limits interfacial charge transfer, and therefore photoelectric conversion efficiency.^{8–13} Band unbending can also influence carrier dynamics near the surface, and this effect is strongly coupled to the surface minority carrier trapping event.^{8,14–16} Consider an n-type GaAs photoanode in depletion which is excited by a short pulse of light through the Schottky barrier interface. Minority carriers are immediately accelerated to the semiconductor surface and provide a compensating charge which will tend to diminish the surface potential. In the absence of minority carrier trapping or interfacial charge transfer at the surface, the minority carriers are expected to survive in the valence band with a lifetime approximately equal to the bulk minority carrier lifetime, which for n-GaAs is on the order of 10 ns.¹⁷ Under this assumption, one would not expect band unbending to occur until a very high injection rate was achieved. For a surface potential of 0.1 eV, a compensation charge of about 6×10^{11} minority carriers/cm² is required to flatten the bands,¹⁷ and these carriers must be generated within 10 ns, requiring an injection rate of about 10^{20} carriers/cm²/s. In the presence of surface midgap states, this situation can change significantly. Surface recombination via midgap states is often assumed to be a facile process which is independent of system parameters such as excitation power and applied potential.^{18–20} Under these circumstances, the surface is a sink for minority carriers, and band unbending is difficult to achieve because the facile loss mechanism increases the required injection rate even further. Yet this picture is inconsistent with recent studies of the GaAs/

electrolyte interface,^{16,21–29} which suggest that the detailed kinetics of surface recombination has a significant influence on carrier dynamics near the GaAs/electrolyte surface.

The surface recombination event can be considered a two-step sequential process: (1) trapping of minority carriers by midgap states and (2) recombination of the trapped carrier with a majority carrier.⁸ In this case, one can envision a scenario in which band unbending is achieved at relatively low injection levels. If the rate of the recombination event is slow compared to the rate of the trapping event, the charge-compensating trapped carrier can linger at the surface and its simultaneous influence on carrier dynamics and band unbending (i.e., band edge shifts) endures until the recombination event occurs. In this paper, we present a method which exploits excitation-power-dependent photoluminescence efficiency measurements to examine the kinetics of surface recombination at the GaAs/electrolyte interface. We present an expression for the dependence of the photoluminescence efficiency (PLE) of a semiconductor under short pulse excitation on the surface minority trapping velocity (S) and demonstrate that the functional dependence of the PLE on S is identical to that for CW excitation. Using the method of Chmiel and Gerischer,^{21,24,25} we determine the magnitude of S at the GaAs/Na₂S electrolyte interface at the flat band potential under fixed excitation intensity. Using this value of S at the flat band potential as a point of reference, we determine S versus excitation power from PLE measurements. We then present a model which allows us to estimate the residence time of a minority carrier in a surface trap. Our analysis indicates that the recombination event occurs on a time scale which is nearly 3 orders of magnitude longer than the bulk minority carrier lifetime.

II. Experimental Section

Experiments were performed on the 100 face of n-GaAs ($N_d = 2 \times 10^{17}$ /cm³) immersed in 0.1 M Na₂S/0.1 M KOH electrolyte. Ohmic contact to the backside of the GaAs was

* To whom correspondence should be addressed: chemkauf@showme.missouri.edu.

made by first etching the back surface and then applying InGa eutectic. A copper lead was attached to the contact with silver epoxy, and the contact surface was mounted to a glass tube. The contact was sealed from the electrolyte with Apiezon W wax. The electrode was immersed in a Teflon electrochemical view cell with a Pt counter electrode. The GaAs potential was controlled by a three-electrode potentiostat and was measured versus a second Pt reference electrode located as close as possible to the GaAs electrode and poised at the electrolyte potential. The electrolyte potential versus Ag/AgCl is 0.26 V. An open circuit photovoltage of -1 V is observed in the system under the strongest illumination, placing an upper limit on the flat band potential. The flat band potential of GaAs is largely determined by pH and is predicted to have a value of -1.1 V in our system.^{17b} This value is also consistent with Mott–Schottky analysis and analysis of potential-dependent photoluminescence under weak illumination using the dead layer model performed previously in the same system.^{22,23} Variations in the Na₂S concentration demonstrate that the forward bias current is limited by solution conductivity and appears to be nearly linear in concentration near the flat band potential. In 0.1 M Na₂S, the current changes polarity at -0.76 V, and a forward current of about -0.1 mA is observed at -1.1 V. Estimating the series resistance at $1000\ \Omega$ from direct measurements of solution resistance, we anticipate that the surface potential is poorly controlled when the applied potential is within 0.1 V of the flat band potential. A flat band potential of -1.1 V is used for all subsequent analysis.

The excitation source is the 532-nm second harmonic of a mode-locked Nd:YAG laser operating at a repetition rate of 82 MHz. The light source is directed through a variable density filter, a chopper, and a lens onto the sample and has a beam diameter of 0.35 mm at the sample surface. A small portion of the light is directed onto a reference photodiode to monitor the excitation power. All reported excitation powers refer to absorbed laser power which has been corrected for reflections at interfaces. Photoluminescence from GaAs at 840 nm is collected through a monochromator and 740-nm long pass filter and is processed with a lock-in amplifier using a 100 ms time constant. The output of the lock-in amplifier and the reference photodiode are collected with an analogue-to-digital converter and processed with a lab computer. The computer also controls the attenuation of the excitation source via the stepper motor controlled variable density filter. The photoluminescence efficiency is defined as the ratio of the GaAs photoluminescence intensity to the excitation power determined from the reference photodiode. Photovoltammograms are collected at fixed excitation intensity while scanning the GaAs potential. With the exception of Figure 6, all studies were performed on the same GaAs sample on the same day. The data in Figure 6 were collected on a separate sample constructed from the same GaAs wafer, and identical measurement conditions were used. Electrode corrosion resulted in small decreases ($\sim 10\%$) of the observed PL efficiency after multiple potential scans, and the observed effect is exacerbated by the passage of high current under depletion conditions. All excitation power scans were therefore initiated at the lowest power and scanned toward higher power, and all voltage scans were initiated at the open circuit potential and scanned first toward the accumulation regime and then toward depletion. The photovoltammograms displayed in the figures are the first cathodic scans after $+0.5$ V is reached. These steps served to minimize the accumulated influence of localized surface corrosion on PL intensity over the course of a particular power or voltage scan. The sample position was

also changed after each voltage or power scan to avoid accumulated effects over the course of multiple experiments.

III. Photoluminescence Efficiency Model

Several groups^{30–33} have derived the following expression for the decay of semiconductor photoluminescence following delta function excitation:

$$\frac{L(T)}{L(0)} = \left\{ \frac{1}{A} e^{A^2 T} \operatorname{erfc}(A\sqrt{T}) - \frac{1}{S} e^{S^2 T} \operatorname{erfc}(S\sqrt{T}) \right\} \frac{SA}{S-A} e^{-T} \quad (1)$$

(All symbols have the usual meaning and are defined in the Glossary.) Equation 1 assumes implicitly that the semiconductor is maintained under flat band conditions. The dependence of picosecond laser excited photoluminescence intensity on the surface minority trapping velocity is found as the integral over time of eq 1. Using the expression³⁴

$$\int_0^\infty A e^{bx} \operatorname{erfc}(c\sqrt{x}) dx = \frac{A}{b} [(1 - b/c^2)^{-1/2} - 1] \quad (2)$$

the integral of eq 1 over all time can be simplified to an expression of the form

$$I_{\text{PL}} = C' \int_0^\infty \frac{L(T)}{L(0)} = CI_{\text{ex}} \frac{1 + A + S}{(S + 1)(A + 1)} \quad (3)$$

which predicts the dependence of the average rate of photoluminescence from a semiconductor on S and A . The prefactor CI_{ex} reflects two important points. First, we expect the photoluminescence intensity to scale linearly with excitation power (I_{ex}) unless S or A depend on excitation power. Second, the measured photoluminescence intensity depends on numerous experimental details which are expected to be constant over the course of a particular experiment. These factors are contained in the instrument constant C . The photoluminescence efficiency is determined as the ratio of the average photoluminescence intensity to the excitation power, thus

$$\text{PLE} = \frac{I_{\text{PL}}}{I_{\text{ex}}} = C \frac{1 + A + S}{(S + 1)(A + 1)} \quad (4)$$

We note that the functional dependence of the photoluminescence intensity on S for picosecond pulse excited photoluminescence is identical to that predicted for CW excitation after steady state has been achieved.³¹ Figure 1 plots the dependence of the PLE on S according to eq 4 normalized against C , the instrument constant. The figure indicates the expected behavior between the limiting values of $S = 0$ (PLE = 1) and $S = \infty$ (PLE = $(1 + A)^{-1}$). The results are only weakly dependent on the value of A . The plot demonstrates that the PLE is insensitive to S when it approaches 20, and this provides a working definition of the term “effectively infinite surface minority trapping velocity” since values of S which exceed 20 cannot be distinguished from one another. On the other hand, the PLE is extremely sensitive to S for values below 8. The sensitivity of the intermediate S regime ($S = 8$ –20) is somewhat dependent on the value of A , but in all cases the dependence of PLE on S is weak in this regime. Equation 4 holds for excitation conditions under which eq 1 holds. These conditions include flat bands and a low injection rate.^{30–33} To maintain an injection rate which generates a photon density less than 3% of the doping density over a volume equal to the excitation area times the diffusion length ($2\ \mu\text{m}$), the total photon flux should not exceed

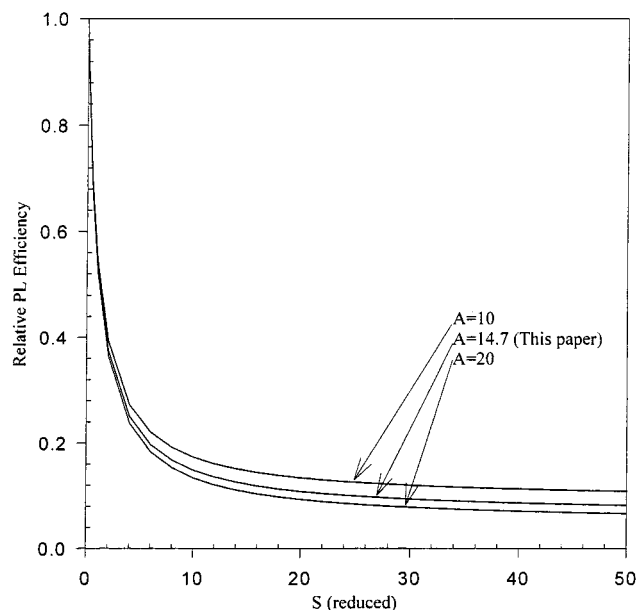


Figure 1. Photoluminescence efficiency versus S (reduced surface minority trapping velocity) predicted using eq 4. Plots for three values of A (reduced absorption coefficient) are presented. The plots have been normalized against the instrument factor, C . In this paper, $C = 7.1$. The value of A used in this study has been calculated as $A = 14.7$ for GaAs under 532-nm excitation.

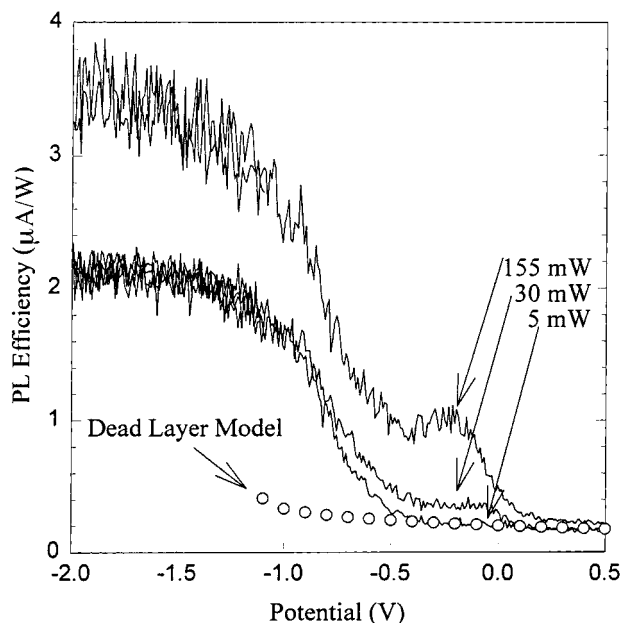


Figure 2. Photovoltammograms measured under several different excitation powers. The open circles are predictions using the dead layer model, eq 5. The difference between this prediction and the measured intensity at the flat band potential (-1.1 V) has been used to calculate the surface minority carrier trapping velocity using the model of Chmiel and Gerischer.²⁵ (See Table 1 and eq 7.)

10^{12} photons/cm² over the minority carrier lifetime. This requires an average photon flux of less than 2×10^{20} photons/cm²/s. We have assumed that neither A nor S depends on time. The validity of this assumption will be clarified in section VI.

IV. Surface Trapping Velocity at the Flat Band Potential

Figure 2 shows photovoltammograms taken on the same GaAs electrode sample using different excitation power densities under otherwise identical conditions. The dead layer model:

el^{18–21,24,25} predicts that the dependence of the photoluminescence intensity in the depletion region on applied bias under a fixed excitation intensity follows the expression

$$I_{\text{PL}} = I_{\text{PL}}^{\infty} \exp(-\alpha W) = I_{\text{PL}}^{\infty} \exp(-0.668 \sqrt{V_{\text{ap}} - V_{\text{fb}}}) \quad (5)$$

The depletion region is assumed to be dead with respect to radiative recombination. The second equality is based on the expression,

$$W = \sqrt{\frac{2\epsilon\epsilon_0 V_s}{qN_d}} \quad (6)$$

using values for the required quantities which are appropriate for our samples.^{17,35,36} Note that we plot the photoluminescence efficiency along the y-axis in Figure 2, and the photovoltammogram traces have not been otherwise normalized to one another. Under the assumption that S and A are independent of intensity, the PLE scans should be identical to one another since the linear dependence of the PL intensity on excitation intensity is divided out in the PLE calculation. Figure 2 shows that this prediction holds under deep depletion, but intensity dependence is observed across the depletion-to-flat-band region. The dead layer model assumes that the surface minority trapping velocity is effectively infinite across the depletion-to-flat-band regime. In applying this model, it is generally assumed that this holds in deep depletion, and therefore the deep depletion photoluminescence intensity can be used as a point of reference in order to compare the model with experimental results. Figure 2 demonstrates the insensitivity of the PLE to excitation power in deep depletion ($V_{\text{ap}} > 0.25$ V), which indicates that this assumption is justified under our conditions. To our knowledge, the validity of this assumption under varying excitation powers has not been previously examined. We have plotted the predictions of the dead layer model in Figure 2 and observe significant deviation between the model and the experimental results at the flat band potential under all excitation conditions. These results are similar to those observed by Kauffman, Balko, and Richmond²³ on identical samples in the same electrolyte and have been attributed to a dependence of S on excitation power. Time-resolved PL decays have demonstrated a dramatic increase in the PL lifetime with increasing excitation power in this system.^{21,22} The increase in lifetime is contrary to the behavior expected for intensity-dependent variation in the radiative rate, and we can rule out this effect. Furthermore, a bulk impurity density of 2×10^{17} and a bulk lifetime of 6.4 ns indicate that an excitation flux of about 10^{25} photons/cm²/s would be required to saturate bulk traps assuming a 2-μm diffusion length. This is far in excess of our highest photon flux. Fouquet and Burnham⁶ have observed bulk impurity state saturation in MOCVD-grown GaAs of low doping density, but the effect is only observed when the photon flux over the lifetime of a bulk carrier exceeds the doping density by nearly an order of magnitude. We therefore attribute the observed excitation-power-dependent variations in the PLE at the flat band potential to intensity-dependent variations in S .

Chmiel and Gerischer²⁵ have derived an expression which allows one to extract the value of the surface minority trapping velocity at the flat band potential from the ratio of the measured photoluminescence efficiency to that predicted by the dead layer model:

$$S = (1 + A - \beta)/(\beta - 1) \quad (7)$$

where $\beta = I_{\text{PL}}^{\text{fb}}/I_{\text{PL}}^{\infty}$. We have performed this calculation for

TABLE 1: Reduced Surface Minority Carrier Trapping Velocities (S) Calculated by the Method of Chmiel and Gerischer²⁵ (Eq 7) under Several Excitation Powers^a

excitn power (mW)	av flux (photons/ cm ² s)	flux per pulse (photons/ cm ² pulse)	S	C	S from ref 23
5	1.4×10^{19}	1.7×10^{11}	3.3	5.0	17
30	8.4×10^{19}	1.0×10^{12}	3.0	8.4	5.8
155	4.3×10^{20}	5.2×10^{12}	1.5	6.4	3.6
290	8.1×10^{20}	9.9×10^{12}	1.3	8.5	

^a The surface minority carrier trapping velocity is calculated by multiplying the reduced value by 3×10^4 cm/s for our samples. The photon fluxes are computed from average powers and parameters given in the Experimental Section. The instrument constant (C) is extracted from the S values using eq 4. For comparison, values of S for similar pulse fluxes from ref 23 are also presented. The reduced values for the results in ref 23 are calculated for the lowest value in the reported range, assuming that $(D/\tau)^{1/2} = 3 \times 10^5$.

each of the excitation powers in Figure 2, and the results are tabulated in Table 1. These results indicate a dependence of the surface minority trapping velocity on excitation power, even at the flat band potential where surface band-to-band recombination should mimic that in the bulk semiconductor. The trend toward lower S values with increasing excitation power is similar to the previous measurements of Kauffman et al.²³ in which the identical system was studied using the Chmiel–Gerischer model. In all cases the S values in the present study are substantially lower than those reported previously at similar photon fluxes per pulse, and we attribute this to the higher pulse repetition frequency used in the present study. We suggest that the reduction in S results from an effective decrease in the number of available (unoccupied) surface traps when high pulse repetition frequencies are used. The analysis presented in section V indicates that the time scale for the surface electron–hole recombination event is much longer than the time between excitation pulses in the present study, and as a result, minority carriers accumulate in surface traps, effectively reducing the value of S . We defer discussion of the anomalous behavior in the -0.3 – 0.0 V region until section VI.

V. Photoluminescence Efficiency at the Flat Band Potential

To further elucidate the kinetics of the surface recombination process, we have measured photoluminescence efficiencies versus excitation power at several applied potentials. These are shown in Figure 3. In the absence of excitation-power-dependent surface minority trapping or absorption coefficient, we expect a linear plot having a slope of zero. Under deep depletion, we observe a relatively flat photoluminescence efficiency curve, indicating that the surface recombination velocity is effectively infinite under this condition. Under depletion, flat band, and accumulation conditions, we observe a PLE curve which varies logarithmically with excitation power. Similar observations have been reported by Sawada et al. for GaAs in a vacuum²⁶ and have been analyzed by consideration of the surface trap density of states. Liu and Kauffman have recently reported a large difference in the PLE plots of bare versus Na₂S-treated GaAs in air.³⁷ The bare sample exhibits only a slight dependence (<2 -fold increase) on excitation power, while the Na₂S-treated sample shows a 30-fold increase over the same excitation power variation. This illustrates the sensitivity of the PLE measurement to the surface trap state density.³⁷ In the current paper, comparison of PLE under depletion versus flat band conditions shown in Figure 3 exhibits a similar variation. These observations are also consistent with

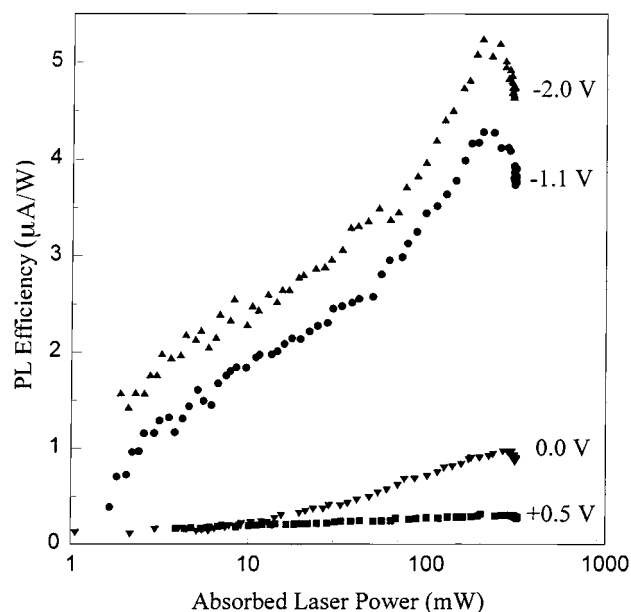


Figure 3. Photoluminescence efficiency plots at several applied potentials. The 0.0 and +0.5 V scans are in depletion, and anodic photocurrent is observed during these measurements. The intensity turnover under strong excitation is a thermal effect. See text for details.

the expectation that the surface minority trapping velocity should be high under deep depletion but may depend on excitation intensity near the flat band potential.

The intensity turnover observed at excitation powers in excess of 200 mW reflects the onset of a thermal effect which we have thoroughly examined in air and in solution.³⁸ The effect reflects heat buildup in the GaAs sample due to poor thermal contact to a heat sink. Stirring of the solution, for example, diminishes this effect. The effect is not observed in our experimental configuration at excitation powers below 200 mW. Apparently, neither the glass rod to which the GaAs electrode is attached nor the quiescent solution in contact with our samples provides a heat sink sufficient to obviate this effect when the excitation power exceeds 200 mW. We limit our subsequent data analysis and discussion to measurements at excitation powers below 200 mW.

Equation 4 allows us to extract the value of S from the PLE intensity at the flat band potential. Using the independent measurements of S from Table 1 at fixed excitation intensity and the calculated value of A in eq 4, we have determined the average value of the instrument constant (C) to be 7.1 ± 1.7 for this set of experiments. Inverting eq 4 gives

$$S = (1 + A - \gamma)/(\gamma - 1) \quad (8)$$

where $\gamma = \text{PLE}(A + 1)/C$. Equating eqs 7 and 8 demonstrates that $\gamma = \beta$, and it can be shown that C is equivalent to the photoluminescence yield constant in the original work by Chmiel and Gerischer.²⁵ Whereas eq 7 was developed under the assumption of a steady-state carrier excitation profile, eq 8 provides an analogous model for short pulse excitation. The equivalence of these results arises from the fact that the functional dependence of the photoluminescence efficiency on S and A is identical for CW and pulsed excitation.

Using eq 8 we have determined S versus excitation power at the flat band potential. The results are shown in Figure 4 along with the PLE measurement at the flat band potential from Figure 3. At an excitation power of 2 mW, the value of S exceeds 20, and the surface minority trapping velocity is effectively infinite. Note that the value of the PLE at this power is about 0.5, which

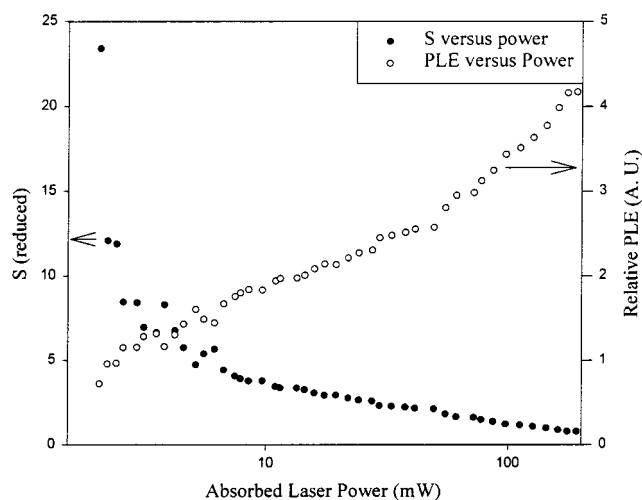


Figure 4. PLE at the flat band potential along with the calculated value of S determined from the PLE using eq 8. The PLE data is the same as in Figure 3.

is the PLE predicted by the dead layer model at the flat band potential (see Figure 2). This indicates that the average instrument constant determined from analysis based on eq 4 provides a reasonable connection between the photovoltammograms and the PLE traces. Note also that the value of S drops dramatically between excitation powers of 2–20 mW and continues to drop albeit more slowly from 20 to 200 mW.

Given the fact that different sample spots and different irradiation times cannot be avoided over the course of the experiment, the agreement between the PLE measured versus potential and excitation power is quite remarkable. Note, for example, that the PLE at under 5 mW excitation power is ~ 1.4 from both the photovoltammogram and the power-dependent PLE measurement. On the other hand, the values of S obtained from the PLE versus power scan differ somewhat ($\sim 30\%$). This arises because we have used an average value of the instrument constant, C , calculated from the results in Table 1 to determine the S values in Figure 4. Variations in the value of C determined using eq 4 are unavoidable due to the modest signal-to-noise ratio of the experiments described here, and this is reflected in the 25% standard deviation of C . Contributions to noise, including source flicker and gas evolution at the electrode interface, are difficult to control. The standard deviation of C characterizes the magnitude of the possible systematic error in its value. Though this issue is cause for concern regarding the precision of the values of S presented in Figure 4, we are still able to draw some general conclusions regarding the influence of excitation intensity on the kinetics of surface recombination in GaAs.

We interpret these results on the basis of the following model. The reduced surface minority trapping velocity can be written as³⁵

$$S = s\sqrt{\tau/D} = v_{\text{th}}\sigma T_s\sqrt{\tau/D} \quad (9)$$

Using the value $\sqrt{\tau/D} = 3 \times 10^{-5}$ s/cm, the density of unoccupied surface traps can be written

$$T_s \text{ cm}^{-2} = (4 \times 10^{12})S \quad (10)$$

and this expression allows us to extract a value for the density of unoccupied surface traps versus excitation power from the values of S in Figure 4. Assuming that the total number of

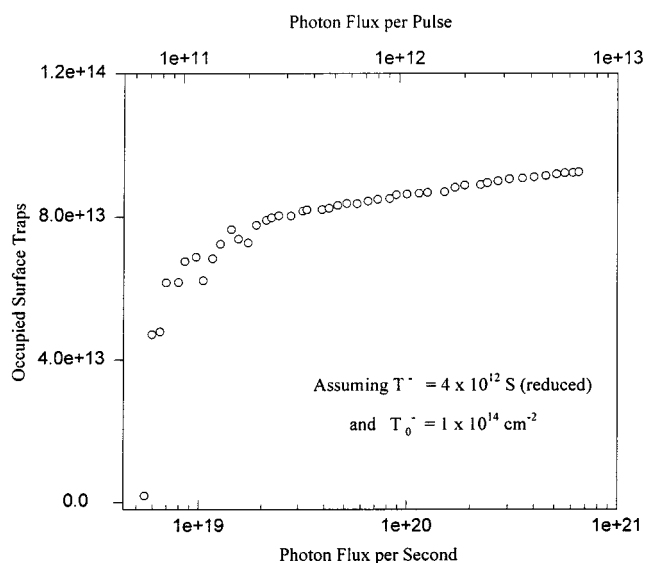


Figure 5. Occupied surface trap density versus photon flux. The density of occupied surface traps is calculated from eq 10 and the calculated values for S shown in Figure 4.

occupied plus unoccupied surface traps is 2% greater than the value calculated at 2 mW ($N_{\text{ss}} = 1 \times 10^{14} \text{ cm}^{-2}$), we can calculate the number of occupied surface traps at a particular excitation power as the difference between the low power value and the value of T_s extracted from eq 10 and Figure 4 for that particular power. This calculation assumes that we achieve a steady-state value for N_{ss} on a time scale which is short compared with the time scale of our measurement. The number of occupied surface traps versus photon flux is shown in Figure 5. Note that the number of occupied surface traps exceeds the number of photons per excitation pulse by almost 2 orders of magnitude. We therefore conclude that the residence time of a trapped minority carrier in the trap exceeds the length of time between excitation pulses by several orders of magnitude.

The ratio of the number of occupied traps given in Figure 5 to the photon flux per second provides a measure of the time duration necessary to generate enough photoexcited minority carriers to fill the calculated number of occupied traps. The calculated time durations are on the order of 10 μs , and this implies that trap state saturation which is responsible for the dramatic dependence of the PLE on excitation power occurs because the trapped holes reside in the trap states for time durations in excess of a microsecond. If the electron–hole surface recombination event were facile, we would be unable to effect a significant change in the PLE at low excitation powers. It appears, however, that surface electron–hole recombination is a relatively slow process which results in surface trap saturation at low photon fluxes and can also lead to band unbending at low photon fluxes due to charge accumulation at the surface (band edge shifting) when a depletion layer exists. The microsecond time scale for electron–hole surface recombination determined from these PLE measurements in bulk GaAs is similar to the carrier decay time scale measured by Yablonovitch et al.³⁵ for ultrapure MOCVD-grown GaAs. This suggests that the mechanism of surface recombination is the same on bulk grown or epitaxially grown samples and that increases in S in the bulk grown sample are the result of an increase in T_s . Balko and Richmond³⁹ have also estimated that the lifetime of a hole in a surface trap is 1–4 μs on the basis of studies of the dependence of photovoltammograms on the pulsed excitation repetition rate.

VI. Discussion

The results of Figure 2 contrast the results of Kauffman, Balko, and Richmond^{21,23} which show good agreement with the dead layer model for photovoltammograms collected using the same photon flux per pulse as in the 5 mW case shown in Figure 2, but with a 150-kHz repetition rate. This comparison emphasizes the fact that surface trap state saturation is dependent upon the average excitation power when the pulse repetition frequency exceeds the inverse of the minority carrier trap state residence time and is consistent with the conclusions of the present study regarding the kinetics of surface recombination. Slow electron-hole recombination following minority carrier trapping will also result in dynamic band edge shifts due to accumulated charge at the semiconductor/electrolyte interface. The results of this study indicate that band edge shifts are unavoidable in the GaAs/electrolyte system. The time scales for the trapping and recombination events suggest that the band edge under illumination will be established on a time scale which will depend on excitation power and will be on the nanosecond to microsecond time scale. On the other hand, the band edge after illumination is turned off relaxes back to the thermodynamic value on a microsecond time scale. These circumstances ensure that a steady state is achieved within a few microseconds after initiating the excitation and that the limiting time constant for establishing the steady-state band edge exceeds 1 μ s.

The photovoltammogram exhibits anomalous intensity-dependent behavior in the -0.3 – 0.0 V region, particularly under high-power excitation. Balko and Richmond have observed similar behavior and have reported that the magnitude of this anomaly increases as the surface is corroded.³⁹ They have suggested that there may be two or more distinct energy regions in the gap in which the surface trap density is high, one of which is attributable to photocorrosion. The excitation power dependence of the anomaly observed in the current work indicates that traps are more easily saturated at -0.25 V than at -0.5 V, which is consistent with the suggestion that two distinct surface trap states are operative, regardless of their origin. We have examined the influence of electrolyte concentration on this behavior, and the results are shown in Figure 6. Photovoltammograms under two different excitation powers in electrolyte at two different concentrations are displayed. We have shifted the x -axis of the high-concentration traces to highlight the similarity between the traces. On the basis of the measured shift of the potential of the reference electrode, we anticipate a negative shift in the flat band potential of about -0.1 V, yet the cusp in the traces characteristic of the flat band region occurs at a potential which is shifted by $+0.25$ V. Though we have not measured the flat band potential of the high-concentration system by independent methods, the characteristic shape of the photovoltammogram near the flat band potential is apparent in the high-concentration traces at a potential of about -0.75 V. Qualitatively, it appears that the high concentration of electroactive electrolyte shifts the band edge at the GaAs/electrolyte interface by about $+0.35$ V. This is not surprising given the strong interaction between sulfides and the GaAs surface. Note that in both high- and low-power traces, the PLE is diminished near the flat band potential as the concentration increases. This indicates that interfacial electron transfer plays a significant role in surface minority carrier trapping. The observed similarity of the high- and low-concentration traces upon shifting is also apparent in the region associated with the anomalous PLE variation (-0.3 – 0.0 V in the low-concentration traces). The magnitude of the anomaly is diminished as the surface trap density increases, whether by increasing the concentration of

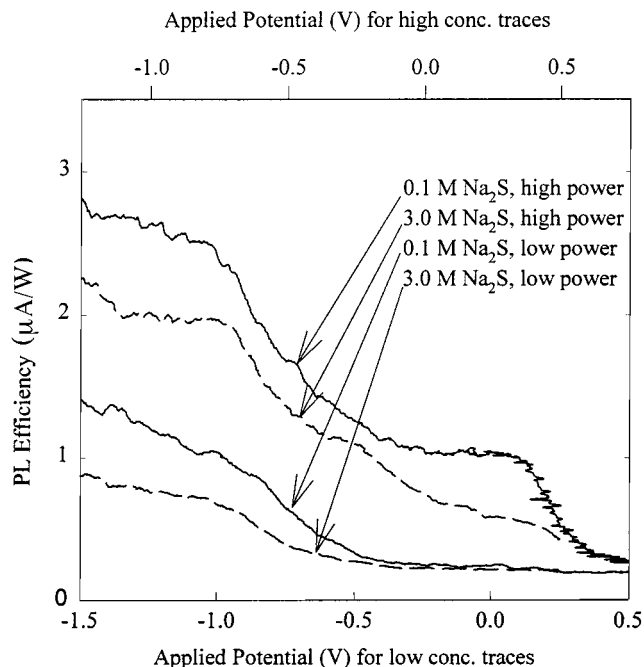


Figure 6. PLE photovoltammograms for GaAs under weak (4.5 mW) and strong (187 mW) illumination. The solid traces are in 0.1 M Na_2S and 0.1 M KOH. The broken traces are in 3.0 M Na_2S and 0.1 M KOH. Note that the high- and low-concentration traces have different x -axes which are shifted by 0.25 V. The similarity between the shifted low- and high-concentration traces suggests that apparent concentration-dependent variations in observed behavior may result primarily from shifts in the reference electrode potential and the semiconductor band edges.

electroactive species in the electrolyte or by reducing the excitation power. These observations are consistent with the conclusions of Balko and Richmond. The 0.0 and $+0.5$ V traces in Figure 3 demonstrate that the excitation power at the onset of the anomaly is about 20 mW. Below this power both depletion regime traces are identical. At powers in excess of 20 mW, a noticeable deviation between the depletion and deep depletion PL characteristics is observed. This may signal the onset of band edge shifting in the 0.0 V trace resulting from minority carrier accumulation at the GaAs/electrolyte interface. Band edge shifts may not be operative in deep depletion where the Fermi level at the surface is located close to the valence band edge in a region of high state density. Such effects will also be minimized near the flat band potential where mobile majority carriers are able to compensate for minority carrier accumulation near the surface. These results suggest that photovoltammetry in the depletion region under high-power illumination may provide a simple method for mapping the density of the surface midgap trap states. Perhaps the most crucial result presented herein is the observation that the functional dependence of the PLE on S is the same for pulsed and CW excitation.³¹ This is particularly important in light of the long residence times for trapped minority carriers determined from the present study and the high pulse repetition frequency used in this study. With respect to surface minority carrier trapping, our results indicate that when using pulsed excitation one effectively makes a transition between pulsed and CW excitation as the pulse repetition frequency increases from the kHz to the MHz regimes. As this transition is made, the fact that the functional dependence of the PLE on S remains constant simplifies the analysis of the results.

Kauffman, Balko, and Richmond²² have examined photoluminescence decay from GaAs/electrolyte junctions and have

interpreted the results in terms of a time-dependent surface minority trapping velocity. The time dependence arises as the result of surface trap filling following short pulse excitation, and the time constant for this process is on the order of nanoseconds. Those studies were performed with a pulse repetition frequency of 150 kHz and demonstrated the influence of a time-dependent concentration of surface traps on the observed surface recombination velocity. Their results are significant within the current context for two reasons. First, the present study verifies that trapped minority carriers have a very long residence time relative to the bulk lifetime, and this is consistent with their observation of a time-dependent minority carrier trapping velocity on the time scale of the bulk lifetime. Second, the present analysis assumes that the reduced minority carrier trapping velocity has no explicit time dependence on the time scale of the measurement. The influence of trap state filling on S occurs on a time scale of roughly 10 ns, whereas the residence time of the trapped minority carrier is on the order of microseconds. We therefore anticipate that a steady-state value for S is achieved within a few microseconds after the excitation intensity is changed, which is instantaneous with respect to our time constant of 100 ms. As a result, the value of S is effectively constant on the time scale of our measurement.

The residence times of trapped minority carriers in surface traps establishes an effective time constant for examination of surface recombination kinetics with pulsed excitation. Pulse repetition frequencies in excess of a few hundred kilohertz result in excitation rates which are fast relative to the relaxation rate of trapped photoexcited minority carriers. Pulse repetition frequencies near 100 MHz such as those used in this study are effectively continuous with respect to surface recombination as a result of the slow rate of surface electron-hole recombination. For a given excitation power density, a steady-state condition will be achieved within a few tens of microseconds, and on the time scale of our measurement, we are effectively always in the steady-state condition.

We have assumed a rather large value for N_{ss} based on eq 10 and values of S extracted from the photovoltammograms. A value of $N_{ss} = 1 \times 10^{14}$ is a factor of 10 larger than expected from intrinsic impurity states on a bare GaAs surface³⁵ and represents about 10% surface coverage with trap states. We can propose two possible explanations for this apparently high value: (1) Our method cannot distinguish between minority carrier trapping by intrinsic surface impurity states and electrolyte states. The high value of N_{ss} may reflect a high surface coverage of minority carrier acceptors in the electrolyte half space. In this case, diffusion of the oxidized electrolyte away from the surface and concomitant diffusion of a reduced ion to the surface constitutes an electron-hole recombination event as far as the GaAs/electrolyte interface is concerned. The time scale for these events is consistent with the values for the residence times of minority carriers at the surface estimated by the present analysis, and the observed dependence of S on electrolyte concentration supports this possibility. (2) The estimates for the minority carrier capture cross section, the value of S , and the thermal velocity at the surface used in eq 10 may differ from true values. In this case, we may simply be using a value for N_{ss} which is too large by perhaps an order of magnitude. If we use a value of $N_{ss} = 10^{13}$ in our analysis, we still find residence times in surface trap states which are on the order of 1 μ s, orders of magnitude longer than the bulk minority carrier lifetime. This circumstance does not affect the qualitative conclusions of the present study regarding surface trap state saturation.

Acknowledgment. This research was supported in part by the National Science Foundation (CHE-9508744) and by the University of Missouri Research Board. The authors wish to thank Mr. Mazdak H. Khajepour for assistance in preparing this manuscript.

Glossary

Definitions of various parameters and values appropriate for the system under study in this paper are given below.

- t = time (s)
- τ = bulk minority carrier lifetime (6.4×10^{-9} s)¹⁷
- s = surface minority trapping velocity (cm/s)
- α = absorption coefficient ($78\,421\text{ cm}^{-1}$ at 532 nm)³⁶
- D = minority carrier diffusion coefficient ($5.5\text{ cm}^2/\text{s}$)¹⁷
- $S = s\sqrt{\tau/D}$ (reduced surface minority trapping velocity)
- $A = \alpha\sqrt{D\tau}$ (reduced absorption coefficient, 14.7)
- $T = t/\tau$ (reduced time)
- $L = \sqrt{D\tau}$ (diffusion length, 1.9×10^{-4} cm)¹⁷
- I_{ex} = excitation power
- I_{PL} = measured PL intensity
- I_{PL}^{∞} = calculated PL intensity at the flat band potential assuming s is infinite
- I_{PLfb} = measured PL intensity at the flat band potential
- V_s = surface potential (V)
- V_{ap} = applied potential (V)
- V_{fb} = flat band potential (-1.1 V in the system under study)
- q = the fundamental charge
- N_d = doping density (cm^{-3})
- ϵ_0 = permittivity of free space
- ϵ = dielectric constant of GaAs (13.1)³⁶
- W = depletion width (cm)
- v_{th} = minority carrier thermal velocity (3×10^7 cm/s)³⁵
- σ = surface trapping cross section (3×10^{-16} cm²)³⁵
- T_s = density of unoccupied surface traps (states/cm²)
- N_{ss} = intrinsic surface trap state density (T_s at equilibrium in the dark)

References and Notes

- (1) Kauffman, J. F.; Richmond, G. L. *Appl. Phys. Lett.* **1991**, *59*, 561.
- (2) Oh, Y. T.; Byun, S. C.; Lee, B. R.; Kang, T. W.; Hong, C. Y.; Park, S. B.; Lee, H. K.; Kim, T. W. *J. Appl. Phys.* **1994**, *76* (3), 1959–1961.
- (3) Sandroff, C. J.; Hegde, M. S.; Farrow, L. A.; Bhat, R.; Harbison, J. P.; Chang, C. C. *J. Appl. Phys.* **1990**, *67* (1), 586–588.
- (4) Manorama, V.; Bhoraskar, S. V.; Rao, V. J.; Kshirsagar, S. T. *Appl. Phys. Lett.* **1989**, *55* (16), 1641–1643.
- (5) Wilmsen, C. W.; Kirchner, P. D.; Woodall, J. M. *J. Appl. Phys.* **1988**, *64*, 3287–3289.
- (6) Fouquet, J. E.; Burnham, R. D. *IEEE J. Quantum Electron.* **1986**, *QE-22*, 1799.
- (7) Marvin, D. C.; Moss, S. C.; Halle, L. F. *J. Appl. Phys.* **1992**, *72*, 1970.
- (8) Gerischer, H. *J. Electroanal. Chem.* **1983**, *150*, 553.
- (9) Mao, D.; Kim, Kang-J.; Frank, A. J. *J. Electrochem. Soc.* **1994**, *141*, 1231.
- (10) Tufts, B. J.; Casagrande, L. G.; Lewis, N. S.; Grunthaner, F. J. *Appl. Phys. Lett.* **1990**, *57*, 1242.
- (11) Rosenbluth, M. L.; Lewis, N. S. *J. Phys. Chem.* **1989**, *93*, 3735.
- (12) Lunt, S. R.; Casagrande, L. G.; Tufts, B. J.; Lewis, N. S. *J. Phys. Chem.* **1988**, *92*, 5766.
- (13) Archer, M. D.; Bolton, J. R. *J. Phys. Chem.* **1990**, *94*, 8028.
- (14) Wada, Y.; Wada, K. *J. Vac. Sci. Technol., B* **1993**, *11* (4), 1598–1602.
- (15) Offsey, S. D.; Woodall, J. M.; Warren, A. C.; Kirchner, P. D.; Chappell, T. I.; Pettit, G. D. *Appl. Phys. Lett.* **1986**, *48*, 475–477.
- (16) Yablonovitch, E.; Skromme, B. J.; Bhat, R.; Harbison, J. P.; Gmitter, T. *J. Appl. Phys. Lett.* **1989**, *54*, 555–557.
- (17) (a) Sze, S. M. *Physics of Semiconductor Devices*, 2nd ed.; Wiley: New York, 1981. (b) Morrison, S. R. *The Chemical Physics of Surfaces*, 2nd ed.; Plenum: New York, 1990.

- (18) Hobson, W. S.; Ellis, A. B. *J. Appl. Phys.* **1983**, *54*, 5956.
- (19) Hoffman, C. A.; Jarasiunas, K.; Gerritsen, H. J.; Nurmikko, A. V. *Appl. Phys. Lett.* **1978**, *33*, 536.
- (20) Ando, K.; Yamamoto, A.; Yamaguchi, M. *J. Appl. Phys.* **1980**, *51*, 6432.
- (21) Kauffman, J. F.; Richmond, G. L. *J. Appl. Phys.* **1993**, *73*, 1912.
- (22) Kauffman, J. F.; Balko, B. A.; Richmond, G. L. *J. Phys. Chem.* **1992**, *96*, 6371.
- (23) Kauffman, J. F.; Balko, B. A.; Richmond, G. L. *J. Phys. Chem.* **1992**, *96*, 6374.
- (24) Smandek, B.; Chmiel, G.; Gerischer, H. *Ber. Bunsen-Ges. Phys. Chem.* **1989**, *93*, 1094–1103.
- (25) Chmiel, G.; Gerischer, H. *J. Phys. Chem.* **1990**, *94*, 1612.
- (26) Sawada, T.; Numata, K.; Tohdoh, S.; Saitoh, T.; Hasegawa, H. *Jpn. J. Appl. Phys., Part 1* **1993**, *32* (1B), 511–517.
- (27) Ramakrishna, S.; Rangarajan, S. K. *J. Phys. Chem.* **1995**, *99*, 12631.
- (28) Kruger, O.; Jung, C.; Gajewski, H. *J. Phys. Chem.* **1994**, *98*, 12653.
- (29) Kruger, O.; Jung, C.; Gajewski, H. *J. Phys. Chem.* **1994**, *98*, 12663.
- (30) 'tHooft, G. W.; van Opdorp, C. J. *Appl. Phys.* **1986**, *60*, 1065.
- (31) Wilson, T.; Pester, P. D. *J. Appl. Phys.* **1988**, *63*, 871.
- (32) Bensaid, B.; Raymond, F.; Leroux, M.; Verie, C.; Fofana, B. *J. Appl. Phys.* **1989**, *66*, 5542.
- (33) Ioannou, D. E.; Gledhill, R. J. *J. Appl. Phys.* **1984**, *56*, 1797.
- (34) This integral is solved by expressing the complementary error function explicitly and inverting the order of integration.
- (35) Yablonovitch, E.; Sandroff, C. J.; Bhat, R.; Gmitter, T. *Appl. Phys. Lett.* **1987**, *51*, 439.
- (36) Palik, E. D., Ed. *Handbook of Optical Constants of Solids*; Academic Press: Orlando, FL, 1985.
- (37) Liu, C.; Kauffman, J. F. *Appl. Phys. Lett.* **1995**, *66*, 3504.
- (38) Liu, C.; Kauffman, J. F., manuscript in preparation. We have examined this effect in real time following step function excitation and observe an exponential decrease in PL intensity which approaches a new steady-state intensity. We have modeled the behavior extensively with the heat equation and have shown that the exponential decay constant and the magnitude of the PL change depend on the rate of heat transfer across the GaAs–heat sink interface. When the rate of heat delivery due to photoexcitation is small compared with that of interfacial heat transfer, sample heating does not occur. Apparently, in the present sample this does not hold when the excitation power exceeds 200 mW.
- (39) Balko, B. A.; Richmond, G. L. *J. Phys. Chem.* **1993**, *97*, 9002.